# LEXR: A low-energy X-ray reflectometer for characterization of ATHENA mirror coatings

**Henriksen, P. L.; Christensen, F. E.; Massahi, S.; Ferreira, D. D. M.; Svendsen, S.; Jafari, A.; Shortt, B.**

*Published in:*
Proceedings of SPIE 11119, Optics for EUV, X-Ray, and Gamma-Ray Astronomy IX

*Link to article, DOI:*
10.1117/12.2528144

*Publication date:*
2019

*Document Version*
Publisher's PDF, also known as Version of record

# LEXR: A low-energy X-ray reflectometer for characterization of ATHENA mirror coatings

P. L. Henriksen, F. E. Christensen, S. Massahi, D. D. M. Ferreira, S. Svendsen, et al.

P. L. Henriksen, F. E. Christensen, S. Massahi, D. D. M. Ferreira, S. Svendsen, A. Jafari, B. Shortt, "LEXR: A low-energy X-ray reflectometer for characterization of ATHENA mirror coatings," Proc. SPIE 11119, Optics for EUV, X-Ray, and Gamma-Ray Astronomy IX, 111191F (9 September 2019); doi: 10.1117/12.2528144

Event: SPIE Optical Engineering + Applications, 2019, San Diego, California, United States

# LEXR: A low-energy X-ray reflectometer for characterization of ATHENA mirror coatings

P. L. Henriksen[a], F. E. Christensen[a], S. Massahi[a], D. D. M. Ferreira[a], S. Svendsen[a], A. Jafari[a]
B. Shortt[b]

[a]DTU Space, Technical University of Denmark, Elektrovej, Bygn. 327, 2800, Kgs. Lyngby, Denmark
[b]European Space Agency (ESTEC), Keplerlaan 1, PO Box 299, 2200 AG, Noordwijk, Netherlands

## ABSTRACT

Qualification of coating performance at the low-energy range of the Advanced Telescope for High Energy Astrophysics (ATHENA) is important to ensure that the mirror coatings satisfy the performance criteria required to meet ATHENA's science objectives. We report on the design, implementation, and expected performance of a state-of-the-art Low-Energy X-ray Reflectometer (LEXR) acquired with the purpose of qualifying the soft energy X-ray performance of mirror coatings for ATHENA. The reflectometer components are housed in a vacuum chamber and utilizes a microfocus Al source with custom made Kirkpatrick-Baez mirrors and W/Si monochromator to produce a collimated beam of 1.487 keV photons. The system has been designed with source interchangeability, allowing reconfiguration to an 8.048 keV reflectometer using a Cu source or other energies with sources such as Fe, Mg, etc. Several mirror samples can be mounted on a motorized stage, and a 2D CCD camera is used to obtain spatially resolved detection.

**Keywords:** LEXR, ATHENA, X-ray optics, X-ray reflectometry, thin-film characterization, X-ray telescopes, grazing incidence, coatings

## 1. INTRODUCTION AND SCIENCE OBJECTIVE

ATHENA is a selected large class mission scheduled for launch by ESA in 2031[1]. The current baseline for the optics is one Wolter-I geometry telescope with 12 m focal length based on the Silicon Pore Optics (SPO) technology developed in Europe[2]. They are required to have high performance in the energy range from 0.3 to 12 keV which is obtained by utilizing mirror substrates coated with a combination of high and low-Z materials. The current baseline coating for ATHENA is an Ir/SiC bilayer design optimized for the energy band in question[3,4]. Previous studies performed at DTU Space have established that the requirement for effective area can be achieved at both 1 keV and at 6 keV using a combination of bilayer coatings and/or linear graded multilayers[5,6]. To achieve these effective area requirements it is necessary that the mirror coatings perform as designed and a detailed understanding of how the mirrors perform in practice at various energies is essential.

X-ray reflectometry (XRR) characterization is a technique used to qualify deposited coatings, yielding information about film thickness, roughness, film morphology, density, etc. Single-energy reflectometers are compact and easy to operate, making them ideal for immediate and follow-up characterization of manufactured X-ray mirrors.

Over past activities, it has become apparent that the processes involved in the production of mirror stacks could affect the coating performance and have a particularly negative effect on the performance of the telescope at low energies[7]. So far, most of the characterization of mirror performance has been done at energies above 3 keV, and an investigation at lower energy is required for a complete mirror performance qualification[7,8]. DTU Space is therefore through ESA acquiring the custom-built LEXR operating at 1.487 keV, the main purpose of which, is to qualify the performance of the optics of ATHENA at low energies for characterization and optimization of thin-film coatings for the ATHENA mission.

Further author information - send correspondence to:
Peter Lindquist Henriksen, e-mail: plihen@space.dtu.dk

Optics for EUV, X-Ray, and Gamma-Ray Astronomy IX, edited by Stephen L. O'Dell, Giovanni Pareschi, Proc. of SPIE Vol. 11119, 111191F · © 2019 SPIE · CCC code: 0277-786X/19/$21 · doi: 10.1117/12.2528144

With the addition of LEXR to our current 8.048 keV reflectometer, DTU Space will have characterization ability at two reference energies at either end of the spectrum of interest for ATHENA. While XRR measurements at 8.048 keV provide useful information on films consisting of multilayer coatings or single layer coatings of a high-Z material, low-Z top layers are largely transparent at this energy and their weak signal will be dominated by the signal from high-density coating layers underneath. LEXR will be able to more accurately distinguish any soft overlayer presence, revealing a more complete picture of film surface behavior. As of July 2019, LEXR has been installed, undergone acceptance testing, and is in the commissioning phase.

As the research on optimal coatings for ATHENA optics evolves so does the need for probing the coatings using various methods and characterizing at different energies to probe different length scales and increase our understanding of how each of the layers in the coating behave. This includes, but is not limited to, how chemical interactions with the atmosphere changes the top layer, how the lift-off and cleaning processes that coated SPOs have to undergo impact the coating itself, and the short and long-term stability of deposited films. Stability of coatings is a crucial parameter, and achieving long-term stability is important to ensuring mission success. Recent studies have shown evolution of both reactively and non-reactively sputtered $B_4C$ leading to degradation of the film[9] so an important use of the reflectometer will be to investigate both short and long-term stability of alternative coating recipes with low-density materials such as C or SIC.

This paper describes the reflectometer design and capabilities. The expected performance, in terms of angular resolution and dynamic range, is determined and simulations of foreseen measurements are shown.

## 2. SYSTEM DESIGN

The reflectometer has been designed by JJ X-ray[10] in collaboration with DTU Space, and built by JJ X-ray using a combination of own and third party parts.

### 2.1 Overview

While higher energy XRR studies may be performed in air, this setup is enclosed in a vacuum chamber to prevent attenuation of the low-energy photons. The X-ray source and two Kirkpatrick-Baez (KB) collimating mirrors are mounted on a flange of the vacuum chamber, and the chamber itself slides over and houses all the other components of the reflectometer. The operating pressure in the vacuum chamber is on the order of $10^{-6}$ mbar. The cylindrical vacuum tank has previously been used for soft X-ray studies[11]. LEXR is designed to operate in the horizontal plane, a sketch of the beam path and main reflectometer components is shown in Figure 1 and Figure 2 shows the relative positions of components in a side-view drawing.

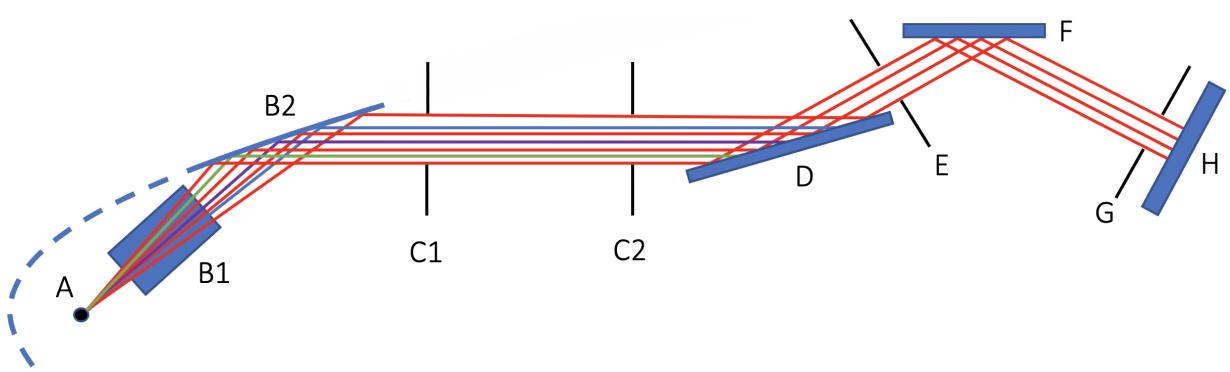


Figure 1: Top down sketch of LEXR beam path. A: A microfocus source emits a bremsstrahlung spectrum along with characteristic photons. B: Two plane-parabolic Kirkpatrick-Baez mirrors collimate the beam in vertical and horizontal plane respectively. C: Slits reduce the level of background. D: A monochromator picks out the $K_\alpha$ line monochromatizing the beam. E: A slit shaping the beam reaching the sample. F: Sample stage holding the X-ray mirror samples. G: Slit reducing the background level. H: 2D CCD Detector.

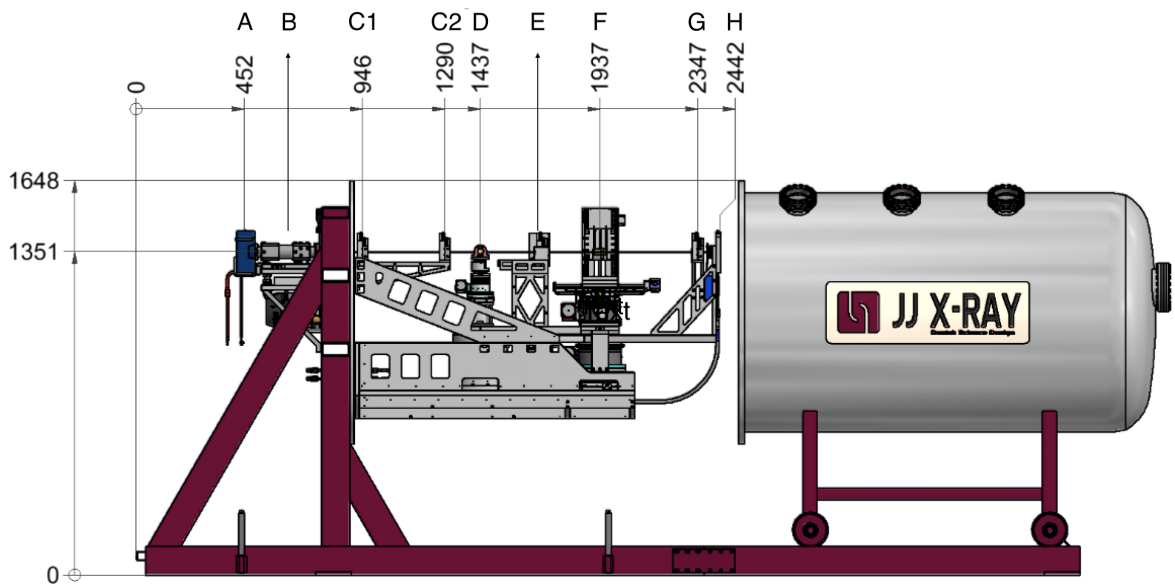

Figure 2: Side-view drawing of LEXR. Measurements given in mm. A: X-ray source, B: Kirkpatrick-Baez mirrors, C: Slits 1 and 2, D: Monochromator, E: Slit 3, F: Sample stage, G: Slit 4, H: Detector.

### 2.2 Sources and mirrors

X-ray sources and mirrors were designed and manufactured by AXO DRESDEN GmbH[12] using X-ray tubes from rtw RÖNTGEN-TECHNIK DR. WARRIKHOFF GmbH & Co. KG[13]. Mirror specifications are given in Table 1. The source assembly comprising the X-ray tube and collimating mirrors, attached to the outside of the vacuum chamber, are adjusted manually as one rigid part with rotations about the three principal axes, as well as vertical and lateral linear motion. Fine alignment of all interior components using the monochromatized beam is done with the position sensitive detector.

The main X-ray source is a microfocus Al source with a spot height of 150 $\mu$m and a spot width of 50 $\mu$m. It may be exchanged with a $70 \times 70$ $\mu m^2$ microfocus Cu source for operation at 8.048 keV. The two KB mirrors, designated M1 and M2, increase the collecting area of photons from the source and collimate the beam from the microfocus source in the vertical and horizontal direction respectively. They have plane-parabolic surfaces coated with laterally graded multilayers optimized for Bragg reflection at Cu $K_\alpha$ and total external reflection at Al $K_\alpha$. As M1 and M2 operate in the total external reflection regime, there are no higher order reflections of Al $K_\alpha$ from their multilayers and the monochromator is designed for optimization of Al $K_\alpha$ flux rather than higher-order suppression. The KB mirrors reflect both Cu $K_{\alpha 1}$ and $K_{\alpha 2}$ so the monochromator must be exchanged with e.g. a Ge crystal when using the reflectometer in the Cu $K_\alpha$ configuration to pick out the 8.048 keV line. Simulations show a combined throughput of 58% for both mirrors using the 70 $\mu$m Cu source.

| Mirror | Source distance [mm] | Multilayer | Multilayer period [nm] | # of bilayers | Deflection angle $2\theta$ |
|---|---|---|---|---|---|
| M1 | 130 | W/Si | 2.99/4.57/5.91 | 60 | 2.1° |
| M2 | 240 | Ni/C | 6.15/6.49/6.83 | 40 | 1.5° |
| Monochromator | 985 | W/Si | 3.75 | 80 | 13.1° |

Table 1: Specifications of mirrors provided by AXO DRESDEN. The multilayer period has a gradient along the KB mirrors, the values stated are nominal at mirror front/center/end respectively.

### 2.3 Motion stages and sample holder

Slits, goniometers, and translation stages are motorized and remotely operated. The monochromator is placed on a goniometer with an angular resolution of 1 millidegree and a linear stage enables positioning with micrometer precision in the beam. The sample stage has linear translation with three degrees of freedom so samples can be moved to intercept the beam reflected from the monochromator, as well as a 360-degree rotational capability to facilitate $\theta$-$2\theta$ scans in different reflectometer configurations. The expected alignment accuracy is 5 $\mu$m in position and 5 mdeg in orientation.

To optimize the number of samples that can be measured between each pump-down cycle, and therefore the science output, a modular sample holder is used to enable the mounting of up to twelve mirror samples at once depending on the sample dimensions (see Figure 3). The standard configuration of the sample holder has plate-to-plate distance of 21.5 mm which, for samples of 1 mm thickness and assuming a 0.5 mm beam, yields sufficient sample illumination up to 17 degrees. For utilization of the full $\theta$-range of the reflectometer or when a larger illumination length on the samples is desired, the sample holder has modularity so the center backplate can be replaced with a distancing piece that still allows for the simultaneous mounting of several samples.

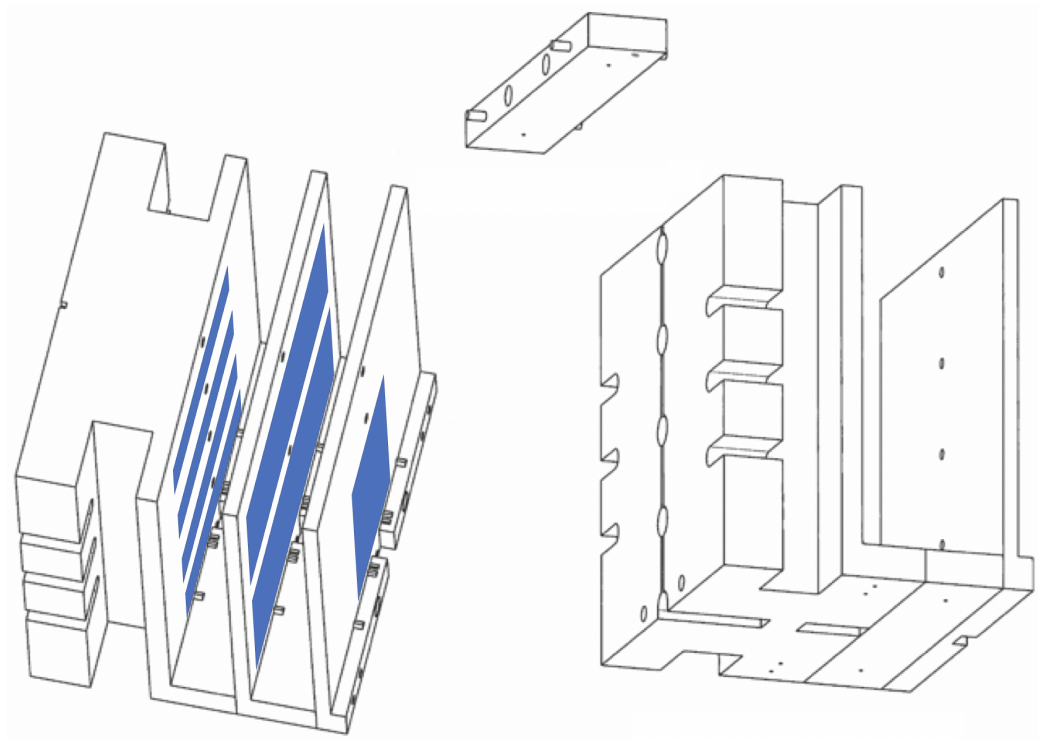

Figure 3: Isometric drawing of modular sample holder. Left: Standard configuration shown with four samples of $70 \times 10$ mm$^2$, two inner radius SPO of $110 \times 49$ mm$^2$, and one $40 \times 66$ mm$^2$ middle radius SPO. Right: Alternative configuration using distancing piece to increase the sample-to-backplate separation.

### 2.4 Detector

The detector is a position sensitive CCD with a 2D resolution of 26 $\mu$m, it is used both for alignment of components and rotation axes in the reflectometer, as well as for data acquisitioning during reflectivity measurements. The detector specifications are listed in Table 2. The detector arm rotates coaxially with the sample stage and the $2\theta$ range is limited to 35° by the chamber wall. Figure 4 shows a typical beam path in the reflectometer.

| Detector specification | Value |
|---|---|
| Pixel format | 1024 × 256 |
| Image area | 26.6 mm × 6.7 mm |
| Pixel size | 26 $\mu$m × 26 $\mu$m |
| Energy range | 10 eV - 11 keV |
| Typ. read noise @ 500 kHz | 9.7 $e^-$ |
| Dark current @ -80 °C | 0.08 $e^-$/pixel/s |
| Quantum efficiency @ 1.487 keV | 0.87 |
| Photoelectrons/photon @ 1.487 keV | 400 |
| Quantum efficiency @ 8.048 keV | 0.45 |
| Photoelectrons/photon @ 8.048 keV | 2000 |

Table 2: Specifications of greateyes GE-VAC 1024 256 BI DD detector[14]. Although the detector has a larger image area, slit 4 limits the throughput to a 7 × 7 mm$^2$ area.

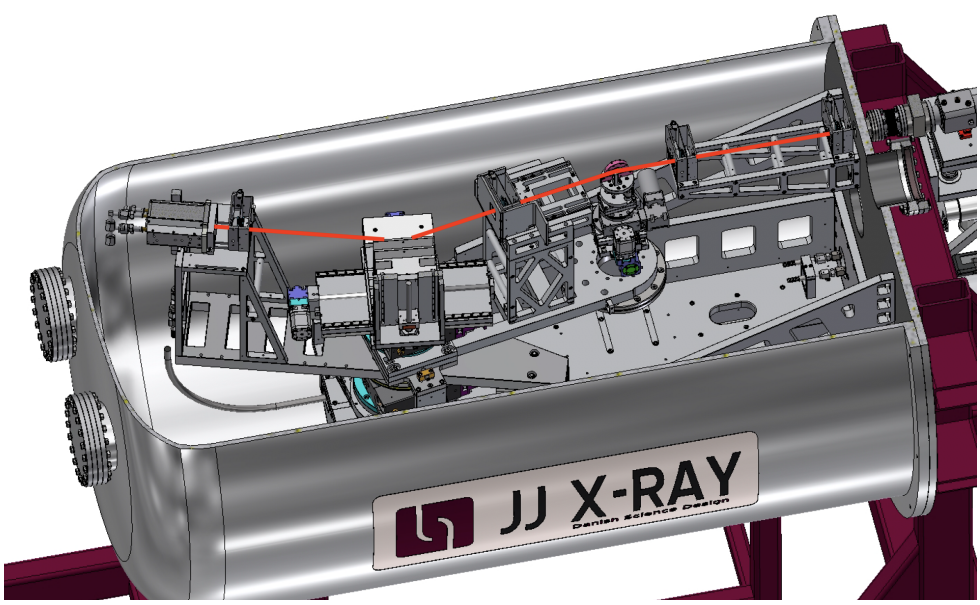


Figure 4: Typical beam path in reflectometer. The beam enters the vacuum chamber from the source assembly (top right), passes through a series of slits and is monochromatized before reflecting off a sample and impinging upon the detector (top left). The detector is here illustrated in the maximum position $2\theta = 35°$.

## 3. REFLECTOMETER PERFORMANCE

### 3.1 Angular resolution

Horizontal and vertical divergence from M1 and M2 with the Al source is

$$\Delta\theta_{\mathrm{M1,vert}} = \frac{0.15 \times 180 \times 60}{130\pi} \approx 3.967'. \tag{1}$$

$$\Delta\theta_{\mathrm{M2,hor}} = \frac{0.05 \times 180 \times 60}{240\pi} \approx 0.716'. \tag{2}$$

which agrees with Monte Carlo X-ray raytracing simulations performed by AXO DRESDEN. Slit 1, reducing the level of background, is placed 494 mm from the source. The second slit is placed 344 mm from slit 1. These slits are both adjusted to 0.5 × 2 mm$^2$ which is the size of the beam coming from the KB mirrors. With these slit openings they do not further reduce beam divergence. From Bragg's law, a relationship between beam divergence and line broadening may be found, here calculated using the fact that the monochromator is optimized for Bragg reflection of Al $K_\alpha$ at 6.54 degrees and assuming the experimentally obtained Al $K_\alpha$ line width $\Delta E \approx 0.85$ eV[15].

$$m\lambda = 2d\sin\theta \Rightarrow m\frac{d\lambda}{d\theta} = 2d\cos\theta. \tag{3}$$

$$\Rightarrow \quad d\theta\frac{\lambda}{d\lambda} = \tan\theta_{B,K_\alpha} \Leftrightarrow \Delta\theta = \frac{\Delta\lambda}{\lambda}\tan\theta_{B,K_\alpha}. \tag{4}$$

$$\theta_{B,K_\alpha} = 6.5^\circ \Rightarrow \Delta\theta \approx 13.6''. \tag{5}$$

The Darwin width (FWHM) at 1.487 keV of the monochromator is $\zeta_D \approx 8.1$ arcmin. The angular acceptance at which a beam of this energy is reflected is thus the convolution

$$\Delta\theta_{\mathrm{monochromator}} = \sqrt{(\Delta\theta_{B,K_\alpha})^2 + (\zeta_D)^2} \approx 8.1'. \tag{6}$$

With a horizontal beam divergence of 0.72 arcmin determined by the KB mirrors, this monochromator does not alter the angular resolution of the system. If the position sensitivity capability of the detector is used for e.g. scatter measurements, an angular resolution of 0.74 arcmin is obtained by convoluting the beam divergence with the resolution dictated by sample-to-detector distance and pixel pitch.

Slit 3 may be positioned 0–220 mm in front of the sample stage meaning any opening wider than 0.3 mm will not further reduce horizontal divergence. A 0.5 mm opening is going to be used for the 1.487 keV measurements. With this divergence a suitable angular step size when measuring specular reflectance is about 10 mdeg.

### 3.2 Dynamical range

The expected flux of $K_\alpha$ photons from the Al source is around $5 \times 10^7$ photons/s after M1 and M2. The monochromator has a reflectance of 1.487 keV photons of around 49% and with a opening of slit 4 of $0.5 \times 2$ mm$^2$ it allows around 91% of the beam through. In front of detector are two filters of 100 nm $Si_3N_4$ + 100 nm Ti to filter out visible light. The combined throughput of these filters at 1.487 keV is around 78%.

The expected number of photons hitting the detector in the free beam (without mirror samples in place) is thus around $1.74 \times 10^7$ photons/s. At this flux, a pixel read-out frequency of 500 kHz is sufficient which has a typical read noise of 9.7 e$^-$. When the detector is cooled to $-80$°C, the dark current is 0.08 e$^-$/pixel/s so when cooled properly and unless exceedingly large exposure times are used, of the total noise, which is the geometric sum of the two, the read-out noise is by far the dominant contributor.

If slit 4 is set to the beam size of 0.5 × 2 mm$^2$, with a pixel size of $26 \times 26$ $\mu$m$^2$ there are ∼1540 pixels exposed so an integration time of e.g. 3 seconds will result in a total noise of $\sim 1.5 \times 10^4$ e$^-$. Each absorbed 1.487 keV photon generates about 400 photoelectrons and the detector quantum efficiency is 87% at this energy so a flux of $1.74 \times 10^7$ photons/s yields a S/N $\approx 1.2 \times 10^6$. This ratio scales almost linearly with exposure time as the dark noise is a subordinate noise contributor. Using the Cu source and operating the reflectometer at 8.048 keV, the dynamical range should be about an order of magnitude larger.

## 4. REFLECTOMETER PERFORMANCE SIMULATIONS

### 4.1 ATHENA baseline coating scans

Reflectivity curves simulated using the IMD software[16] are shown in Figure 5. Simulations show expected $\theta$-$2\theta$ reflectivity curves at 1.487 and 8.048 keV of samples with three different coating designs. The former ATHENA baseline coating consisting of 10 nm Ir with an 8 nm boron carbide layer is shown alongside the current baseline of 10 nm Ir with a 4 nm SiC layer as well as a single layer of 10 nm Ir. A $\theta$-$2\theta$ measurement at 8.048 keV would show only a small difference in reflectivity of the three designs as the low-Z top layers are largely transparent at higher energies. A similar measurement at 1.487 keV will show larger variation in the Kiessig fringe amplitude making characterization of soft material coatings possible.

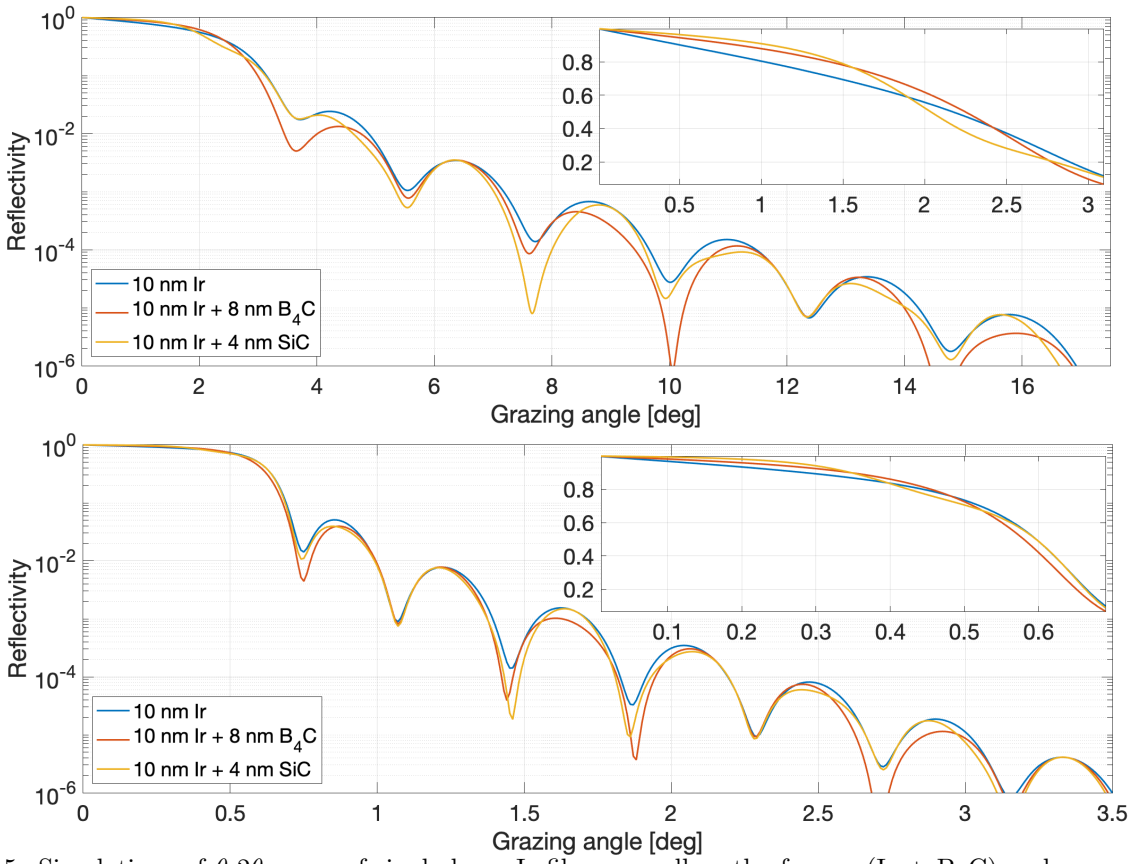


Figure 5: Simulations of $\theta$-$2\theta$ scans of single layer Ir films as well as the former (Ir + $B_4C$) and current (Ir + SiC) ATHENA baseline coatings at 1.487 keV (top) and 8.048 keV (bottom). Inserts show a close-up of the critical angle on a linear scale, note how the critical angle changes at 1.487 keV with the addition of a low-Z top layer. All simulations done assuming SPO rms roughness of 4.5 Å and coating rms roughness of 4 Å.

The soft-overlayer-induced shift in critical angle at low-energy measurements facilitate identification of the presence of surface contaminants such as hydroCs. By transporting newly coated mirrors directly from the coating chamber into the vacuum chamber of LEXR, time stability of e.g. boron carbide thin-films outside atmospheric conditions can be studied. In addition to $\theta$-$2\theta$ measurements, rocking curve scans can be performed to study the surface morphology of the coatings. Combining 1.487 keV measurements of the non-specular reflectance with similar measurements at higher energies provides further insight into interface roughness structures at various length scales.

### 4.2 X-ray source spectrum

The combined reflectance at the center positions of the two collimating KB mirrors and the monochromator has been simulated by AXO DRESDEN along with the spectrum emitted by the aluminium source at both 20 kV and 30 kV. These are shown in Figure 6 along with the transmission spectrum of the two filters installed in front of the detector[17]. The simulations were done with a 30 eV bin width.

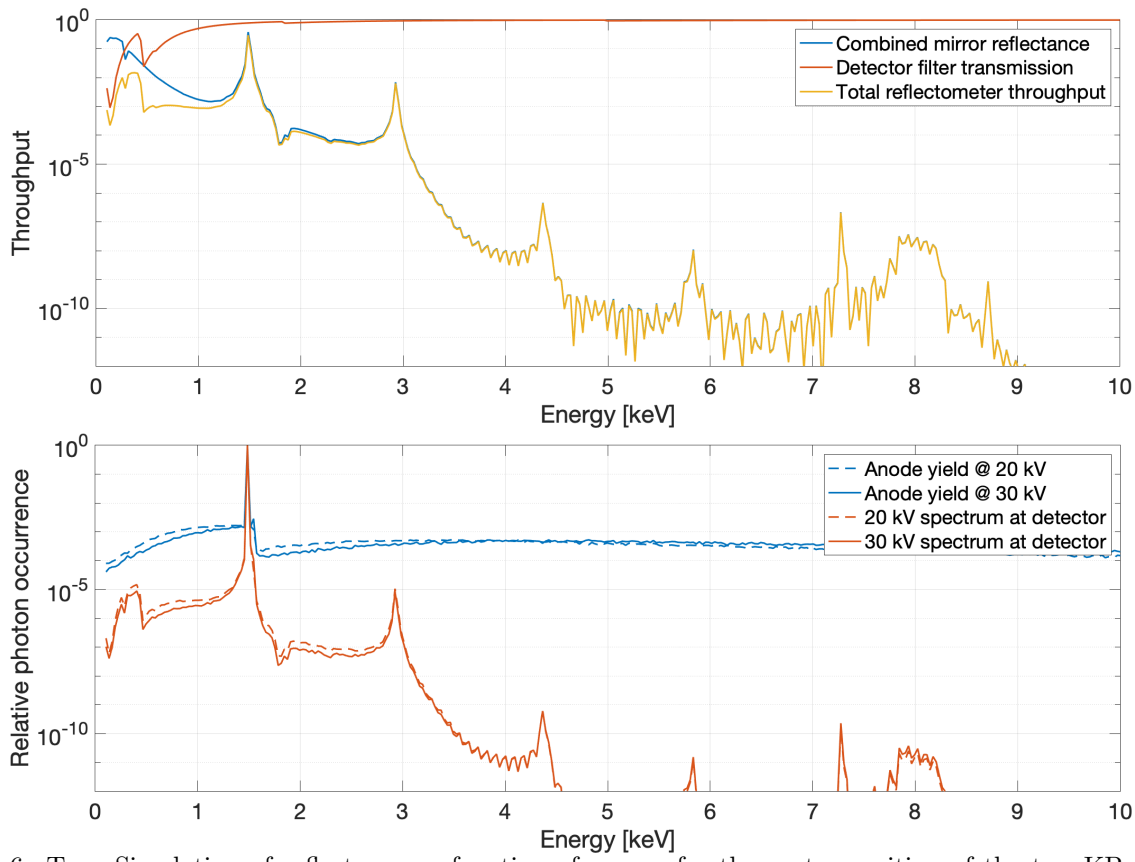


Figure 6: Top: Simulation of reflectance as function of energy for the center position of the two KB mirrors and the monochromator. Combined with the transmission through absorption filters placed at slit 4, the total throughput to the detector is determined.
Bottom: Simulations of the total anode yield of the Al source running at 20 kV and 30 kV respectively. With the total component throughput given above, the resultant spectra at the detector are obtained.

The bremsstrahlung background level is slightly lower when the source operates at 30 kV. This is due to the large penetration depth of the electrons at this voltage so even though low-energy photons are generated, many are absorbed in the anode material as their generation depth is lower than the mean free path of the photons at the given energy in Al. A small peak can be observed at the Al $K_\beta$ edge but due to the electron configuration of Al, few $K_\beta$ photons are generated and the monochromator reduces the amount of these to around 0.1% of $K_\alpha$-photons. The combined mirror reflectance shows $n$th order Bragg peaks from the monochromator as well as a Bragg structure around 8 keV where the KB mirrors are optimized for Cu $K_\alpha$ reflection. The purity of the 1.487 keV beam impinging on the detector is 99.92%.

## 5. SUMMARY

We reported on the design and acquisition of a custom-built low energy X-ray reflectometer to aid in the research and development of thin-film coatings for the ATHENA optics. In addition to the standard 1.487 keV Al source, LEXR can be equipped with other sources to facilitate measurements at different energies. Characterizing coatings at several energies is crucial in ensuring that the effective area requirements for ATHENA are met. With better than arcmin resolution, beam purity above 99.9%, and dynamic range of more than 6 orders of magnitude, LEXR will be used to gain new information on low-density coating behavior and performance.

## 6. ACKNOWLEDGEMENTS

This activity has been funded by the European Space Agency under contract 4000102248/10/NL/PM.

## REFERENCES

[1] Centre national d'études spatiales (July 2019). https://athena.cnes.fr/en/athena-0.

[2] M. J. Collon, G. Vacanti, R. Günther, A. Yanson, N Barriere, et al. Silicon pore optics for the ATHENA telescope. *Proceedings of SPIE*, 9905, 2016.

[3] D. D. M. Ferreira, S. Svendsen, S. Massahi, et al. Performance and stability of mirror coatings for the ATHENA mission. *Proceedings of SPIE*, 10699, 2018.

[4] S. Svendsen, S. Massahi, D. D. M. Ferreira, F. E. Christensen, A. Jafari, P. L. Henriksen, B. Shortt, M. Collon, B. Landgraf, D. Girou, M. Krumrey, L. Cibik, and A. Schubert. Performance and time stability of Ir/SiC X-ray mirror coatings for ATHENA. *Proceedings of SPIE*, 11119, 2019.

[5] D. D. M. Ferreira, F. E. Christensen, A. C. Jakobsen, et al. Coating optimization for the ATHENA+ mission. *Proceedings of SPIE*, 8861, 2013.

[6] S. Massahi, D. D. M. Ferreira, F. E. Christensen, B. Shortt, D. A. Girou, et al. Development and production of a multilayer-coated x-ray reflecting stack for the Athena mission. *Proceedings of SPIE*, 9905, 2016.

[7] D. D. M. Ferreira, A. C. Jakobsen, S. Massahi, et al. X-ray mirror development and testing for the athena mission. *Proceedings of SPIE*, 9005, 2016.

[8] D. D. M. Ferreira, S. Massahi, F. E. Christensen, et al. Design, development, and performance of X-ray mirror coatings for the ATHENA mission. *Proceedings of SPIE*, 10399, 2017.

[9] S. Massahi, F. E. Christensen, D. D. M. Ferreira, et al. The effect of nitrogen incorporation in boron carbide and iridium thin films. *Proceedings of SPIE*, 10699, 2018.

[10] JJ X ray A/S. www.jjxray.dk.

[11] F. E. Christensen, A. Hornstrup, P. Frederiksen, P. Grundsøe, S. Henrichsen, E. Jacobsen, P. Jonasson, M. M. Madsen, C. Nilsson, H. W. Schnopper, N. J. Westergaard, and P. Ørup. Studies of Multilayers and Thin-Foil X-Ray Mirrors Using a Soft X-Ray Diffractometer. *Journal of X-ray Science and Technology*, 2, 1990.

[12] AXO DRESDEN GmbH. www.axo-dresden.de.

[13] rtw RÖNTGEN-TECHNIK DR. WARRIKHOFF GmbH & Co. KG. www.rtwxray.de.

[14] greateyes GmbH. *Data Sheet: GE-VAC 1024 256 Bi DD.*

[15] P. Citrin, P. M. Eisenberg, and W.C. Marra. Linewidths in x-ray photoemission and x-ray emission spectroscopies: What do they measure? *Phys Rev B 10*, 1974.

[16] D. Windt. IMD—Software for modeling the optical properties of multilayer films. *Computers in Physics*, 12(4):360–370, 1998.

[17] B. L. Henke, E. M. Gullikson, and J. C. Davis. X-ray interactions: photoabsorption, scattering, transmission, and reflection at E=50-30000 eV, Z=1-92. *Atomic Data and Nuclear Data Tables*, 54, 1993.